LEGIBILITY NOTICE

CONF-8908134--8

LA-UR--89-3438

DE90 002381

TITLE *Optical Design and Performance of an XUV FEL Oscillator*

AUTHOR(S) *John C. Goldstein, Brian D. McVey, and Brian E. Newnam*

SUBMITTED TO *Proceedings of the 1989 FEL Conference to be published in Nucl. Instr. and Meth. in Phys. Res.*

Optical Design and Performance of an XUV FEL Oscillator*

John C. Goldstein, Brian D. McVey, and Brian E. Newnam

Group X-1, MS E531
Los Alamos National Laboratory
Los Alamos, NM 87545
(505)-667-4370
(505)-665-3389 (FAX)

ABSTRACT

A study by numerical simulation of the performance of a multifacet metal mirror ring resonator FEL is presented for several XUV wavelengths. Laser performance in the presence of mirror aberrations and thermal distortion is calculated for two different output coupling methods, a scraper mirror and a hole.

I. Introduction.

Our previous theoretical work (see [1] and other references therein) has explored the electron beam quality, mirror reflectivity, and wiggler magnet properties needed for an XUV free-electron laser (FEL) oscillator. A ring resonator based on multifacet metal mirrors has been proposed and studied [1] in the context of estimates of available electron beam quality made more than two years ago. More detailed accelerator modeling has been recently done [2] which is partially based upon an improved understanding of the optimum beam transport conditions for the special kind of electron beam generated by a photocathode injector [3, 4]. We use the beam quality calculated in [2] with updated estimates of available mirror reflectivities to predict the performance of XUV oscillators at four different wavelengths: 100 nm, 50 nm, 12 nm, and 4 nm. Two alternative outcoupling schemes are considered in these studies: a scraper in the back leg of the ring, and a hole in one of the metal mirror facets.

We next present some results on the performance degradation induced by spherical aberration on one of the mirrors of the ring. This represents a first attempt to characterize the tolerable level of mirror aberrations in these devices. In this study of static aberrations,

* Work performed under the auspices of the U.S. Department of Energy and supported by a Los Alamos Program Development Initiative.

we limit ourselves to third order spherical aberration only. We examine possible approaches to compensate for the deleterious effects of such aberrations.

A particularly important source of optical aberration in these devices may be thermal distortion of the mirrors due to the high incident optical flux levels and the large mirror absorption coefficients at short wavelengths. We give results of a preliminary study of the effects of the thermal distortion of the mirrors on the operation of these XUV FELs.

II Simulations of XUV FEL Performance.

A schematic layout of the ring optical resonator used in all of the simulations is shown in Fig. 1. The resonator consists of two multifacet metal end mirrors [5] separated by a distance of about 29.5 m. Each mirror has 6 facets, 5 of which are flats and one of which is paraboloidal. The curved elements are the second elements of two beam expansion telescopes in which two grazing angle-of-incidence reflectors, each located 10 m from the center of the wiggler which is placed in the bottom leg of the resonator as shown in Fig. 1, are the other elements. The curvatures of the paraboloids can be varied to vary the Rayleigh range of the lowest order empty cavity Gaussian mode. The Rayleigh range is typically chosen to be about one-half of the wiggler's length. The wiggler's length varies with the optical wavelength in the four cases studied, as does the reflectivity of the multifacet mirrors. Recently, the expected increase in reflectivity with large angles of incidence has been confirmed experimentally [6]. Outcoupling from the resonator is accomplished either with a scraper mirror placed in the middle of the back leg, or with a hole placed in the first flat mirror of the downstream reflector. The round trip optical path length in the unloaded resonator is almost exactly 60 m; the width of the resonator is 1.37 m and is not drawn to scale in Fig. 1.

The laser performance was evaluated with the 3-D FEL simulation code FELEX [7, 8, 9]. The 3-D motion of electrons in the wiggler — including energy spread and finite transverse emittance — is included in FELEX, as is the diffraction of light. The code does not do the full 3-D treatment of reflections from nonnormal-incidence mirrors; rather, the optical elements are treated as thin lenses. All calculations are for a single wave front, i.e., a single frequency; pulse effects are not included. Quoted values of optical power should be regarded as peak powers since the peak value of the current was used in the simulations.

However, the possibility of higher power due to the development of the sideband instability must be considered for any device with a sufficiently large small-signal gain to cavity loss ratio. All quoted results are steady-state values from multiple-pass, self-consistent, full-resonator solutions.

The electron beam parameters are taken from [2]. We have actually used beam quality values 50% less than those of [2] for the 100 nm and 50 nm cases; we used the full values for the 12 nm case. For the 4 nm case, an electron beam which approaches the highest quality conceivable from a photocathode/linac system was needed. This case should be regarded as more speculative than the other three cases in which the beam quality was obtained from very complete simulations of the accelerator in [2].

All of the oscillators considered in this study use the same basic type of wiggler, but in different lengths according to the required gain. The basic wiggler parameters are: wavelength $\lambda_w = 1.6$ cm; magnetic field strength $B_w = 0.75$ T; dimensionless vector potential $a_w = 1.12$; and curved pole faces for two-plane focusing.

(A). Results for the 100 nm Oscillator

The electron beam parameters are: mean energy 184.46 Mev ($\gamma = 361.685$); peak current $I = 300$ A; fractional energy spread $\delta\gamma/\gamma = 0.155\%$; and "90%" normalized transverse emittance $\epsilon_n = 31\ \pi$ mm-mr. The reflectance of each multifacet metal mirror is 90%. The empty cavity Rayleigh range is 1.5 m. The wiggler length is $L_w = 3$ m. The threshold gain (from mirror reflectivity losses alone) is 1.28.

The calculated results are: maximum small-signal gain of 11.21 at an optical wavelength $\lambda = 100.05$ nm. The steady-state power output was calculated for various scraper and hole sizes for outcoupling. Maximum output power was found to be 58 MW with a scraper of radius 0.575 cm. Lower output powers were obtained with hole coupling because the hole caused the optical mode to diverge through the wiggler and thus to be considerably larger than the optical spot in the wiggler using the scraper mirror.

(B). Results for the 50 nm Oscillator.

The same electron beam parameters, except a different energy, were used for this case as for the 100 nm oscillator: mean energy 261.4 Mev ($\gamma = 511.5$); $I = 300$ A; $\delta\gamma/\gamma = 0.155\%$; $\epsilon_n = 31\ \pi$ mm - mr. The reflectance of each multifacet metal mirror is 70%; the empty cavity Rayleigh range is 2 m. The wiggler length is $L_w = 5$ m. The threshold gain is 2.1163.

The maximum small-signal gain was found to be 12.0 at $\lambda = 49.96$ nm. A maximum output power of 21.5 MW was found with hole coupling using a hole of radius 0.225 cm. Scraper mirror output did not exceed 14.5 MW for any scraper mirror radius.

(C). Results for the 12 nm Oscillator.

The electron beam parameters are: mean energy 534.3 Mev ($\gamma = 1045.62$); I = 300 A; $\delta\gamma/\gamma = 0.1\%$; $\epsilon_n = 23.4\ \pi$ mm - mr. The reflectance of each multifacet metal mirror is 60%. The empty cavity Rayleigh range is 5 m. The wiggler length is $L_w = 12$ m, and the threshold gain is 2.88.

A maximum small-signal gain of 14.04 at $\lambda = 11.94$ nm was calculated. A steady-state maximum output power of 9.5 MW was achieved with hole coupling and a hole radius of 0.0578 cm.

(D). Results for the 4 nm Oscillator.

The electron beam parameters are: mean energy 919.8 Mev ($\gamma = 1800$); I = 400 A; $\delta\gamma/\gamma = 0.1\%$; $\epsilon_n = 10\ \pi$ mm - mr. These values are at the upper bound of conceivable beam quality from a photocathode/linac system. The reflectance of each multifacet metal mirror is 35%: this value reflects theoretical projections using material constants for a multilayer dielectric, but as yet measured values have not exceeded about 20%. The empty cavity Rayleigh range in the simulation is 6 m, and the wiggler length is $L_w = 12$ m. These parameters give a threshold gain of 8.465.

The simulations produced a maximum small-signal gain of 14.3 at $\lambda = 4.026$ nm. A maximum power output of 4.89 MW was found with hole coupling and a hole radius of 0.0263 cm.

III. Effects of Spherical Aberration on the Performance of XUV FELs.

We have introduced third order spherical aberration into the phase front of the light via the Zernike polynomial [10] Z13 in the following way: the optical phase ϕ is written as $\phi = \phi_0 + (2\pi\alpha/\lambda)$ Z13, where α is the magnitude of the aberration in waves and Z13 = $6\rho^4 - 6\rho^2 + 1$. Here $\rho = r/r_n$, where r_n is a "normalization radius" which defines the actual radial scale of the aberration. We calculated the effects of introducing the aberration only at the first paraboloidal facet of the downstream multifacet reflector. This is the sixth facet of that mirror in the direction of propagation of the light. All other optical elements of the resonator were taken to be ideal.

We have reached the following two conclusions: (1) The scale size r_n is crucial; if r_n is much larger than the optical spot size on the paraboloidal facet, the magnitude of the aberration is small over the optical beam radius and the effects are small. We calculated for the 50 nm oscillator that, for $\alpha = 0.5\ \lambda$ and $r_n = 4$ cm, the output power was reduced by one half relative to the unaberrated case. For $r_n = 2.46$ cm, which is three times the optical spot size in the unaberrated case, the output power was reduced by a factor of 0.15. (2) For r_n = three times the unaberrated spot size, we found for all four XUV wavelengths of this study that an amplitude of 0.2λ reduced the output by a few percent, 0.5λ reduced the output by a large factor (70%-85%), and 1.0λ prevented laser action entirely.

The above results were obtained by putting various amounts of aberration into the wave front. One might expect that one could make changes to various elements of the resonator to attempt to compensate for the presence of the aberration. We report here the results of such attempts. Since one effect of the aberrated mirror is to increase vignetting losses, we reduced the outcoupling in an attempt to recover the ideal system total cavity loss. We found a small improvement in the case of 0.5λ of spherical aberration, but this method did not succeed at all with 1.0λ of spherical aberration.

We then tried to compensate for the aberration by refocusing the curved mirrors according to the following strategy: the radius of curvature of the first paraboloid was changed so as to recover, approximately, the same spot size on the second paraboloid as in the unaberrated case; the curvature of the second paraboloid was changed so as to recover, approximately, the same Rayleigh range of the light after reflection from that mirror as in the unaberrated case. We found that this scheme worked well for a modest aberration (0.5λ with $r_n = 4$ cm for the 50 nm oscillator) in the sense that almost the full power output of the unaberrated case was recovered in steady-state. We have yet to try to compensate for the aberration by leaving the radii of curvatures of the paraboloids unchanged but slightly moving their positions so as to accomplish the same beam adjustments of the strategy. We believe that this will prove to be a successful method of aberration compensation as well.

Note that the magnitudes of spherical aberration in this discussion are added to the phase front of the light after reflection from a mirror at oblique angles of incidence. The relationship of these magnitudes to errors on the mirror surface involves various functions of the angle of incidence [11].

IV. Preliminary Results on the Effects of Thermal Distortion.

In the examples studied in Sec. II, the mirrors' absorption coefficient is approximately one minus the reflectivity. The absorption per facet ranges from 1.74% to 16%. Because these figures are very large, nonuniform heating of the mirrors by the nonuniform incident optical flux may be substantial: the resulting surface distortion will also distort any light reflected by the surface. Thermal distortion of the mirrors is expected to be a potentially serious problem for XUV lasers.

Thermal distortion of silicon mirrors subjected to a fixed incident optical flux is presently being calculated by R. D. McFarland, J. H. Vernon, and M. E. Marshall at Los Alamos. Calculations have been performed for the 12 nm oscillator assuming an axially-symmetric optical beam of specified intensity incident on the mirror. The non-normal incidence of the real multifacet mirror is not an axially symmetric problem, but, as a first attempt, it has been approximated by averaging the power absorbed from an elliptical footprint over a circular spot. The thermal calculations assume a Gaussian absorbed intensity distribution on the mirror, and they produce as results plots of the vertical displacement, d, of the mirror surface as a function of radius. The displacement function $(2d/\lambda)$ is then expanded in a series of Zernike polynomials, and so introduced into FELEX.

We have reached the following qualitative conclusions from a preliminary study of this problem: (1) The radial scale size is always about the same as the incident optical spot size (significant lateral spreading does not occur); (2) It appears that any coefficient in the Zernike expansion must be smaller than 0.5λ (in the reflected wave front, not the surface figure) in order not to extinguish the laser; (3) Increasing the number of mirror facets may be an effective way to reduce the absorbed power and, hence, the thermal distortion effects.

V. Summary and Conclusions.

We have calculated the output power of FEL oscillators at four XUV wavelengths using electron-beam and mirror reflectivity data believed to be achievable at this time. Steady-state peak output powers, from multiple-pass, self-consistent, resonator simulations using the code FELEX, were found to be: 58 MW at 100 nm, 21.5 MW at 50 nm, 9.5 MW at 12 nm, and 4.9 MW at 4 nm.

We have made a preliminary study of the effect of third-order spherical aberration on one of the paraboloidal mirrors of the ring resonator. In general, 0.5λ reduces the output very substantially, and 1.0λ extinguishes the laser totally. These aberration magnitudes are in the phase front of the wave normal to the direction of propagation; defects on the mirror surface which lead to this aberration are reduced in their effect on the wave by the cosine of the angle of incidence (here, 75 degrees). We have proposed a mode-matching technique, by either recurving or repositioning the mirrors, to compensate for the aberration and restore the performance to the unaberrated level.

We have started to study the effects of thermal distortion of the mirrors due to the large absorption of XUV mirrors. Thermal expansion calculations have been done to predict surface distortion, and that distortion has been included in FELEX as phase front distortion. These effects, which may be particularly serious at the shorter optical wavelengths, might be substantially reduced by increasing the number of facets of the multifacet metal retroreflector mirrors.

References

1. "Conceptual Designs of a 50 nm FEL Oscillator and a 20-40 nm SASE Amplifier," J. C. Goldstein, B. D. McVey, and C. J. Elliott, Nucl. Instr. and Meth. in Phys. Res. A272, pp. 177-182 (1988).
2. "New Photoelectric Injector Design for the Los Alamos National Laboratory XUV FEL Accelerator," B. E. Carlsten, to be published in Nucl. Instr. and Meth. in Phys. Res. in the proceedings of the 1988 FEL Conference.
3. "Photoelectric Injector Design Code," B. E. Carlsten, to be published in the Proceedings of the 1988 Linear Accelerator Conference held in Williamsburg, VA, October, 1988).
4. "Photocathodes in Accelerator Applications," J. S. Fraser, R. L. Sheffield, E. R. Gray,

P. M. Giles, R. W. Springer, and V. A. Loebs, Proceedings of the 1987 IEEE Particle Accelerator Conference, IEEE catalog number 87CH2387-9, p. 1705 (1987).

5. "Multifacet, Metal Mirror Design for Extreme Ultraviolet and Soft X-Ray Free-Electron Laser Resonators," B. E. Newnam in *Laser Induced Damage in Optical Materials: 1985*, NBS Special Publication 746, H. E. Bennett, A. H. Guenther, D. Milam, and B. E. Newnam, Eds., pp. 261-269.
6. "Reflectance of Aluminum Reflectors in the Extreme Ultraviolet," M. L. Scott in *Short Wavelength Coherent Radiation: Generation and Applications*, Vol. 2, R. W. Falcone and J. Kirz, Eds. (Opt. Soc. Am., Washington, D.C., 1988), pp. 322-324.
7. "Three-Dimensional Simulations of Free-Electron Laser Physics," B. D. McVey, Nucl. Instr. and Meth. in Phys. Res. A250, pp. 449-455 (1986).
8. "Numerical Simulations of Free-Electron Laser Oscillators," B. D. McVey, J. C. Goldstein, R. L. Tokar, C. J. Elliott, S. J. Gitomer, M. J. Schmitt, and L. E. Thode, to be published in Nucl. Instr. and Meth. in Phys. Res. in the proceedings of the 1988 FEL Conference.
9. "Simulation Codes for Modeling Free-Electron Laser Oscillators," J. C. Goldstein, B. D. McVey, R. L. Tokar, C. J. Elliott, M. J. Schmitt, B. E. Carlsten, and L. E. Thode in *Modeling and Simulation of Laser Systems*, Donald L. Bullock, Editor, Proc. SPIE 1045, pp. 28-35 (1989).
10. Principles of Optics, M. Born and E. Wolf, fifth edition (Pergamon Press, NY, 1975), pp. 767-772.
11. "Optical Figure Requirements for Laser Mirrors Used at Oblique Incidence," H. E. Bennett in *Laser Induced Damage in Optical Materials: 1982*, H. E. Bennett, A. H. Guenther, D. Milam, and B. E. Newnam, Eds. (Natl. Bur. Stand., Wash. D.C., 1984) NBS Special Publication 669, pp. 228-233.

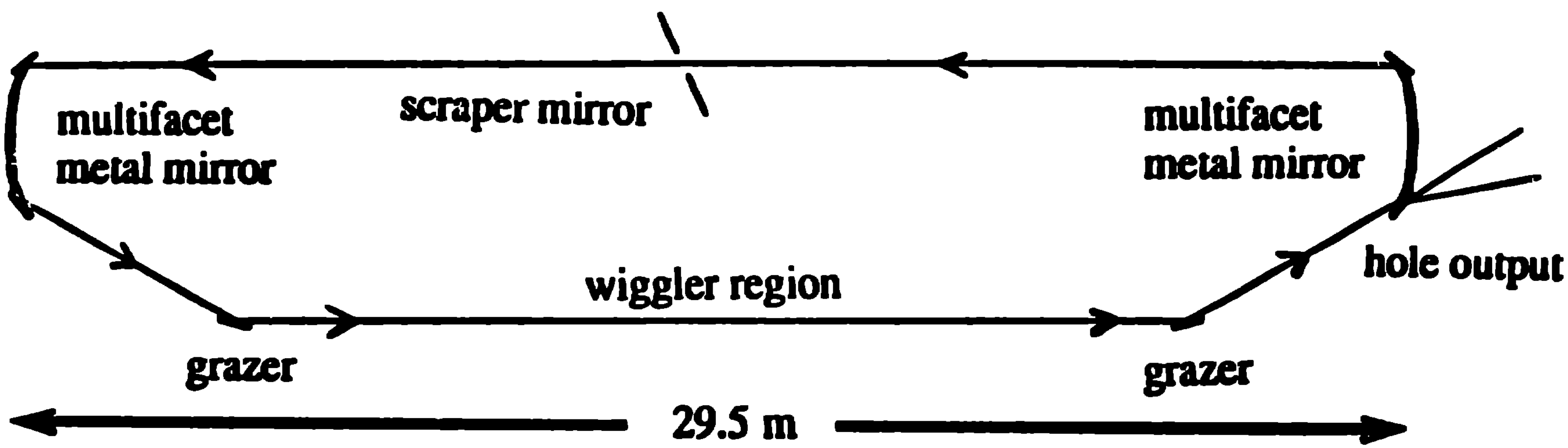
multifacet
metal mirror
scraper mirror
multifacet
metal mirror
hole output
wiggler region
grazer
grazer
29.5 m

Figure 1